COBEM 2021 26th International Congress of Mechanical Engineering
November 22-26, 2021, Virtual Congress, Brazil

COB-2021-0149
CFD ANALYSIS OF A SHELL AND TUBE HEAT EXCHANGER AS THERMAL ENERGY STORAGE UNIT

Diogo do Carmo Zidan
Caio Almeida Friche Passos
Diogo Vilaça Teixeira
Pontifícia Universidade Católica de Minas Gerais
Mechanical Engineering Department
diogo.zidan@sga.pucminas.br
caio.friche@gmail.com
diogo.v.teixeira@hotmail.com

Dr. Ing. Robert Pietzsch
Schmalkalden University of Applied Sciences
Mechanical Engineering Department
r.pietzsch@hs-sm.de

Dr. Cristiana Brasil Maia
Pontifícia Universidade Católica de Minas Gerais
Mechanical Engineering Department
cristiana@pucminas.br

Abstract. *Technological evolution, together with the growth of the world population, has increased the world energy demand. By seeking a solution based on renewable energy sources, energy storage systems using shell-and-tube heat exchangers are indicated as a feasible and low initial investment option. This unit consists of filling the region between the shell and tube with a phase change material (PCM). Through the exchanger tube, flows a heat transfer fluid (HTF). The system charging stage is based on heat injection into the exchanger through the HTF, causing the fusion of the PCM, which, because of its high latent heat, is able to store this introduced energy. A three-dimensional numerical model of a heat exchanger is developed using a smooth tube and it is pursued to improve the thermal performance of the exchanger by the application of circular and helical fins. The CFD analysis, performed using the ANSYS-Fluent 19.0 software, of the three tube configurations, confirms the performance improvement when inserting fins into the tube, making the PCM reach its melting temperature about 2000 seconds faster and thus increasing the melting percentage up to 16.76% after the 9000 seconds of simulation. Thereby, it is concluded that the heat exchanger using circular finned tube presents the best performance and is the most suitable for practical applications, due to its ability to achieve total melting of the PCM in less time and reach higher temperatures, besides being simpler to manufacture when compared to the heat exchanger with a helical finned tube.*

Keywords: *Shell-and-tube heat exchanger, Phase Change Material, CFD analysis*

1. INTRODUCTION

The increase in energy consumption caused by population growth together with the continuous process of industrialization is a reality that covers the whole world. Data presented by the United Nations (UN) estimates the world population of 2020 at 7.794 billion and is expected to reach about 10.151 billion in 2060 (United Nations, 2019). These numbers directly imply an increase in energy demand, and to meet this need, fossil fuels are still the most widely used solution, representing in 2017 about 85.1% of the world's energy matrix (Ruhe, 2019). Consequently, this intensive use of non-renewable energy contributes to increase environmental pollution. According to IEA (International Energy Agency, 2019), around 32.84 million tons of CO2 was emitted worldwide, and the WHO (World Health Organization, 2018) states that air pollution is among the three main factors causing illness and death.

In order to reduce dependence on fossil fuels and thus reduce the environmental impact of their activities, the paper (Woolley et al., 2018) mentions two basic options: the use of renewable energy systems or the reduction of energy consumption. However, according to (Obiwulu et al., 2020; Yang et al., 2019), renewable energy installations require a high initial investment, besides certain climatic and geographical characteristics. Therefore, the scientific community is encouraged to carry out studies focused on energy storage systems.

The importance of storing thermal energy appears in different engineering areas, especially in situations where there is a need to connect the production of this energy to its final demand. Therefore, different methods of storing thermal energy are used. The review carried out by (Cárdenas and León, 2013) points out three of these methods: storage of sensitive heat; storage of latent heat, and thermochemical storage.

Latent heat thermal energy storage (LHTES) systems, using phase change materials (PCM), have been evaluated for various applications. The recent work (Crespo et al., 2019) studies LHTES systems using PCM employed in food and chemical industries, seeking to solve the incompatibility of the energy generated in a solar field to reach its final utility. Fadl and Eames conducted an experimental investigation of an energy storage system using a container filled with paraffin wax RT44HC as PCM, applied for domestic water heating (Fadl and Eames, 2019). To analyze the economic viability, numerical simulations are performed involving tube-hull heat exchangers in LHTES attached to parabolic solar collectors (Bai et al., 2015), and the results highlight this unit as a promising method to reduce the cost of thermal energy storage.

Several authors have also studied the application of PCM in photovoltaic panels, intending to regulate the temperature of cells and maximize their electrical efficiency. Waqas and Li affirmed that panels integrating PCM are capable of reducing cell temperature from 64ºC to 42ºC, increasing the electrical efficiency by 9% (Waqas and Ji, 2017). The experimental research (Yang et al., 2018), which investigated a photovoltaic/thermal (PV/T) panel, confirmed that by attaching a layer of PCM on the lower side of the panel it was possible to reduce the heat loss to the environment and improve the total efficiency of solar energy conversion by 12.94%.

Looking for a solution for sustainable construction, Saxena et al. experimentally examined the behavior of bricks incorporated with PCM during the summer in New Delhi. The study revealed that these bricks have the ability to reduce the temperature from 5ºC to 6ºC compared to normal bricks (Saxena et al., 2019). The numerical investigation (Bhamare et al., 2020) studied the implementation of a PCM layer on the roof of a building. Simulations using the weather conditions of January Chennai showed that the PCM layer inclined by 2º reduced the roof temperature by 2.38ºC.

From the necessity of storing and transporting energy in the form of heat, Guo et al. aimed to analyze the investment required to use shell-and-tube heat exchangers and PCM as mobilized thermal energy storage (M-TES). Supplied with wasted heat in industries, the system proved to be efficient and the return of its initial investment would be in up to 10 years (Guo et al., 2017). Another work (Li et al., 2013) also studied the economic viability of the M-TES system and concluded that the cost-benefit of this unit is directly proportional to the transport distance and inversely proportional to the amount of heat to be transported.

Seeking to improve the effectiveness of a heat exchanger, Cabezas-Gómez et al. presented a theoretical analysis of a new crossflow arrangement comprehending several-tube rows. The work (Cabezas-Gómez et al., 2012) concluded that the uniformity of the temperature difference field led to a higher thermal performance of the heat exchanger. The recent experimental investigation (Shen et al., 2019) confirmed an upgraded thermal performance of a shell-and-tube heat exchanger filled with PCM RT60, with the use of multiple tubes. Fornarelli et al. analyzed, in a theoretical and numerical way, the time necessary for complete fusion of the PCM in a shell-and-tube heat exchanger varying the ratio between the external and internal radius of the exchanger. Keeping constant the volume of stored PCM and the heat transfer area, the ratio of 1.5 presented the shortest load time (Fornarelli et al., 2019). The work (Yagci et al., 2019) examined the influence of the length ratio from the upper and lower edge of the shell-and-tube heat exchanger longitudinal fins. The results showed that the upper edge with 0 mm and the lower edge with 40 mm, the melting time of PCM is significantly reduced in comparison with the other three arrangements, however, the effect proved insignificant during solidification. Mehta et al. experimental study, intended to find the heat exchanger angulation that would result in the shortest PCM charging time. Varying the inclination from 0º to 90º, the experiment concluded that the shortest time is achieved with the system positioned at 45º (Mehta et al., 2019).

Several articles are found in the literature presenting the use of PCM in heat exchangers; on the other hand, few perform three-dimensional numerical analyses evaluating the impact of fins on the performance of shell-and-tube heat exchangers. This work aims to fill this gap in the literature. It presents a shell-and-tube heat exchanger using PCM as an energy storage unit, in which circular and helical fins are applied to improve the thermal performance of the heat exchanger and to evaluate its capacity to decrease the PCM melting time. The numerical model of the smooth tube heat exchanger was compared with experimental data from the work of Hosseini et al. (Hosseini et al., 2014). The analysis was performed using the CFD technique through the ANSYS-Fluent 19.0 computer code. The heat exchanger with better performance and more appropriate for practical applications is defined.

2. SYSTEM DESCRIPTION

The LHTES unit analyzed consists of a shell-and-tube heat exchanger, in which its internal space is filled with PCM. Through its internal tube, a heat transfer fluid (HTF) flows at a rate of 1L/min and inlet temperature set at 70ºC. In this way, the injected heat is absorbed and stored by the PCM, which passes from the solid to the liquid state, as its temperature increases.

The shell-and-tube heat exchanger is engineered using SolidWorks software. It is composed of two concentric tubes, both 1 m long. The inner tube is 22 mm in diameter and 2.5 mm thick. The outer tube is 85 mm in diameter. These specifications are selected according to the experimental model (Hosseini et al., 2014).

The tube with circular fins is designed using 31 fins with 10 mm high, 0.776 mm thick, and 31.3 mm spacing. This configuration is recommended (Yang et al., 2017), in order to maximize the thermal performance of a shell-tube heat exchanger and to minimize the melting time of the PCM. The dimensions of the tube with a helical fin are based on the characteristics of the tube with circular fins. Therefore, the helical fin is arranged with 31 revolutions, 10 mm high and 0.776 mm thick.

Then, the project is imported to the Design Modeler platform of ANSYS 19.0 to finish the creation of the numerical model, establishing the volume of PCM inside the shell and the flow of HTF inside the tube.

The material selected for the heat exchanger tube is copper. The paper (Permatasari and Yusuf, 2018) numerically evaluated a shell-and-tube heat exchanger using steel, aluminum, and copper as materials for the tube, and due to its high thermal conductivity, copper is indicated as the most appropriate material.

The operating principle of the PCM is to absorb and store energy by changing its physical state. Recent work (da Cunha and de Aguiar, 2020) pointed out the problems of applying phase change by evaporation, indicating the solid-liquid transition as a favorite for thermal energy storage, since they do not present a significant change in its volume. Cabeza et al. highlighted a high latent heat and good thermal conductivity as important characteristics for PCM, but Oró et al. mentioned further requirements to be considered, such as (Cabeza et al., 2011; Oró et al., 2013):

- Physical requirements: adequate phase change temperature, reproducible phase change or cycle stability, little under-cooling, no phase separation;
- Technical requirements: low vapor pressure, small volume variations, chemical stability of PCM, compatibility of PCM with other materials and safety restrictions;
- Economic requirements: development of a saleable product, low price, and good reusability.

Experimental tests (Zondag et al., 2018), concluded that the PCM RT70 presented a stable performance and obtained a thermal power of 5 kW during the load phase, while the MgCl2-6H2O obtained only 3.5kW. Recent works (Gorzin et al., 2019; Pahamli et al., 2017) evaluated the effects of nanoparticle dispersion on PCMs applied in shell-and-tube heat exchangers, and the results showed a significant improvement of their heat exchange capacity and reduction of their melting time. Therefore, from the considerations presented, the paraffin RT50 from Rubitherm GmbH is selected for this study.

HTFs are the fluids responsible for transferring heat during the energy charging and discharging phase of the exchanger. Researches, presented in the literature (Qazi, 2017; Wang, 2019), list air, water, synthetic oil, and molten salt as most used HTFs by reason of their low viscosity, high thermal capacity, and low cost. The present study selects water as HTF, not only because it meets the mentioned characteristics, but also because it is easy to replace and clean.

3. MATHEMATICAL MODEL

The following considerations are made for the elaboration of the system's mathematical model:

- The fusion of the PCM is transient and established as a three-dimensional phenomenon;
- The movement of the PCM in the liquid state is considered laminar;
- The effects of compressibility and viscous dissipation are negligible;
- The paraffin RT50 and water are modeled as fluids;
- The HTF inlet into the exchanger tube is set at 70ºC and a rate of 1 L/min.

As an initial condition, all unit is at a temperature of 25ºC. As a boundary condition, the system is considered thermally isolated, so the lower and outer walls are set as adiabatic. Figure 1 shows the system's configuration in the ANSYS-Fluent 19.0 software, where the mentioned conditions are established:

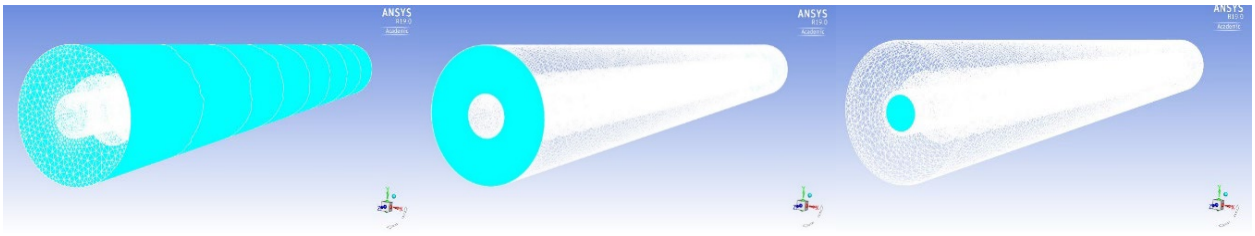

Figure 1. Boundary conditions established for each numerical simulation.

In order to reproduce the charging process of the PCM, CFD simulations are carried out to solve the governing equations, which are based on the conservation of mass, conservation of momentum, and conservation of energy (Versteeg and Malalasekera, 2007):

Mass conservation:

$$\frac{\partial \rho}{\partial t}+\frac{\partial(\rho u)}{\partial x}+\frac{\partial(\rho v)}{\partial y}+\frac{\partial(\rho w)}{\partial z}=0 \tag{1}$$

Momentum conservation:

$$\rho\left(\frac{\partial u}{\partial t}+u\frac{\partial u}{\partial x}+v\frac{\partial u}{\partial y}+w\frac{\partial u}{\partial z}\right)=-\frac{\partial P}{\partial x}+\mu\left(\frac{\partial^2 u}{\partial x^2}+\frac{\partial^2 u}{\partial y^2}+\frac{\partial^2 u}{\partial z^2}\right)+S_x \tag{2}$$

$$\rho\left(\frac{\partial v}{\partial t}+u\frac{\partial v}{\partial x}+v\frac{\partial v}{\partial y}+w\frac{\partial v}{\partial z}\right)=g_y-\frac{\partial P}{\partial y}+\mu\left(\frac{\partial^2 v}{\partial^2 x}+\frac{\partial^2 v}{\partial^2 y}+\frac{\partial^2 v}{\partial^2 z}\right)+S_y \tag{3}$$

$$\rho\left(\frac{\partial w}{\partial t}+u\frac{\partial w}{\partial x}+v\frac{\partial w}{\partial y}+w\frac{\partial w}{\partial z}\right)=-\frac{\partial P}{\partial z}+\mu\left(\frac{\partial^2 w}{\partial^2 x}+\frac{\partial^2 w}{\partial^2 y}+\frac{\partial^2 w}{\partial^2 z}\right)+S_z \tag{4}$$

Energy conservation:

$$\rho\left(\frac{\partial h}{\partial t}+u\frac{\partial h}{\partial x}+v\frac{\partial h}{\partial y}+w\frac{\partial h}{\partial z}\right)=k\left(\frac{\partial^2 T}{\partial^2 x}+\frac{\partial^2 T}{\partial^2 y}+\frac{\partial^2 T}{\partial^2 z}\right) \tag{5}$$

The terms u, v, and w represent the velocity vector in the x, y, and z-direction. The variable ρ denotes the density, P the pressure, and μ the dynamic viscosity of the PCM, g_y is the gravity acceleration in the y-direction. The enthalpy and thermal conductivity are expressed as h and k respectively. The PCM thermos-physical properties are presented in Table 1 (Nitsas and Koronaki, 2021).

Table 1. Thermo-physical properties of PCM, (Paraffin RT50 - Rubitherm Technologies GmbH)

Parameter	**Value**
Density, solid (ρ_s)	0.88 kg/l
Density, liquid (ρ_l)	0.76 kg/l
Latent heat (L)	160±7.5% kJ/kg
Specific heat capacity (Cp)	2000 J/kgK
Dynamic viscosity (μ)	0.03499 kg/ms
Melting temperature range (T_m)	45-51 °C
Thermal conductivity (k)	0.2 W/mK

When the PCM turn into liquid the effect of natural convection is estimated using the Boussinesq approximation, which is showed in Eq. 6 (Fornarelli et al., 2016; Abdulateef et al., 2017). This model treats density as a constant value in the governing equations, except in the momentum equations, in which the density varies with the temperature and it is calculated taking into account the thermal expansion coefficient (β). The variable ρ_0 states for the PCM density at the melting temperature.

$$\rho=\rho_0\cdot\left(1-\beta\cdot\Delta T\right) \tag{6}$$

The solidification and melting model is based on the enthalpy-porosity technique, which defines the dynamics of the region where both PCM phases coexist (Launder B. E. and B., 2013; Niezgoda-Zelasko, 2016). This zone is considered as a porous zone, and the damping terms of Darcy's law, represented by S_x, S_y e S_z, describe how fast the velocity is reduced to zero when the material solidifies:

$$S_x=\frac{(1-\lambda)^2}{\lambda^3+\varepsilon}A_{mush}\cdot u \tag{7}$$

$$S_y=\frac{(1-\lambda)^2}{\lambda^3+\varepsilon}A_{mush}\cdot v \tag{8}$$

$$S_z = \frac{(1-\lambda)^2}{\lambda^3 + \varepsilon} A_{mush} \cdot w \tag{9}$$

A_{mush} is a constant, defined at 10^6, called 'mushy zone'. This parameter represents the motion resistance provided by the PCM during the phase change. The term ε is a constant with a very small value (in the range of 0.001), established by the software to avoid division by zero (Pu et al., 2020).

The total enthalpy (H) is defined as the sum of the sensitive enthalpy (h) and the latent heat (ΔH):

$$H = h + \Delta H \tag{10}$$

Where,

$$h = h_{ref} + \int_{T_{ref}}^{T} Cp \cdot dT \tag{11}$$

$$\Delta H = \lambda \cdot L \tag{12}$$

The latent heat content of PCM varies between zero (solid) and L (liquid) according to the liquid fraction (λ) of PCM:

$$\lambda = \begin{cases} 0 & ,T < T_{solidus} \\ \dfrac{T - T_{solidus}}{T_{liquidus} - T_{solidus}} & ,T_{solidus} < T < T_{liquidus} \\ 1 & ,T > T_{liquidus} \end{cases} \tag{13}$$

ANSYS Meshing is used to do a mesh analysis and finalize the model creation. The mesh of the smooth tube heat exchangers with circular fins and the helical fin is built with a total of 47472, 1842962, and 1446289 elements respectively.

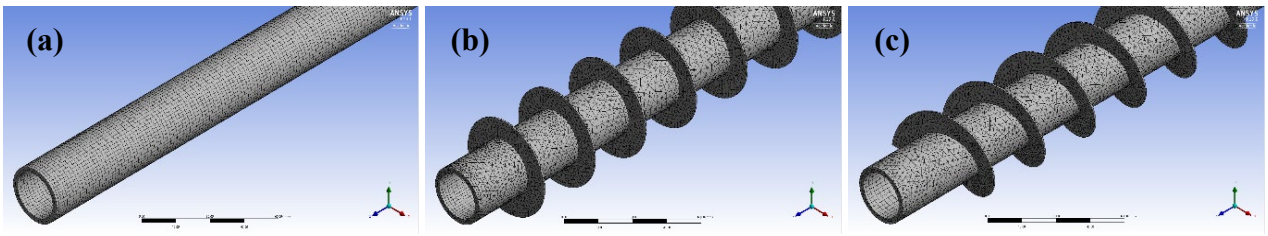

Figure 2. Heat exchangers tubes mesh: (a) smooth tube, (b) tube with circular fins, and (c) tube with helical fin.

To solve the governing equations, the pressure and velocity association algorithm, known as SIMPLE, is applied. For spatial discretization of momentum and energy, the QUICK scheme was established, and for pressure, PRESTO! method was applied. Under-relaxation factors are defined for pressure, density, body forces, momentum, liquid fraction update and energy in 0.3; 1.0; 0.7; 0.9 and 1 respectively. In order to ensure high precision in the results, the waste convergence criteria were specified at 10^{-6}, 10^{-9}, 10^{-9}, 10^{-4}, 10^{-6} for the conservation equations of mass, conservation of momentum in x, y, and z, and conservation of energy respectively.

The three-dimensional numerical simulations, for the three configurations, are performed with a maximum of 200 iterations on each time step. The total simulation time was 9000 seconds, whereas for the heat exchanger using a smooth tube, the time step is 0.1 seconds, and for the heat exchangers using finned tubes, the time step is 0.5 seconds, due to the greater complexity of the geometry. The computer used to run the simulations is a Dell, with a 3.80GHz Intel Xeon processor and 32GB internal memory, taking about 6.83 hours for the smooth tube heat exchanger, 10.58 hours for the circular finned tube heat exchanger, and 14.45 hours for helical finned tube heat exchanger.

4. RESULTS AND DISCUSSIONS

The present work compares the performance of a shell-and-tube heat exchanger with three different configurations: a smooth tube, a tube with circular fins and a tube with helical fins. The data generated from the smooth tube simulation are compared with experimental results taken from literature (Hosseini et al., 2014)).

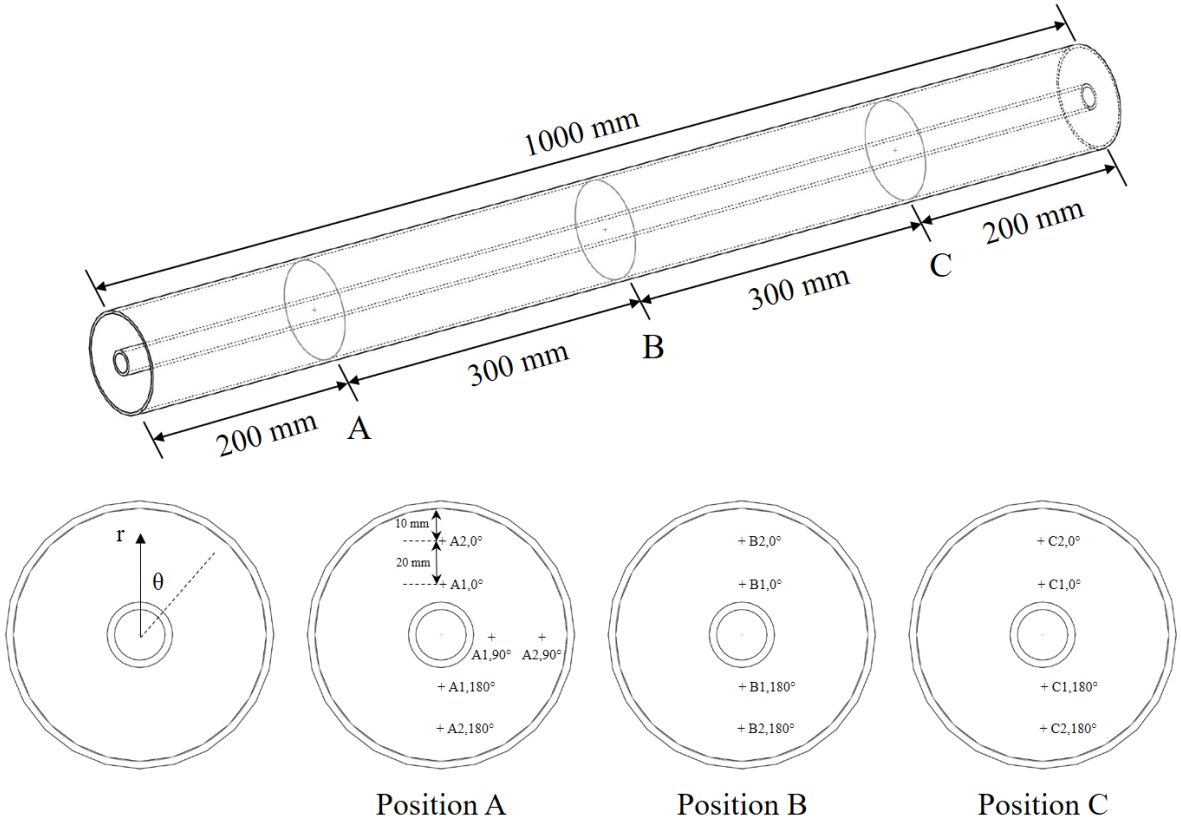

Figure 3. Arrangement of thermocouples used in the experimental model.

The temperature data from the experimental analysis are obtained every minute by the 16 thermocouples distributed along the symmetry axis, in the cross-sections A, B, and C, spaced 10 mm radially in each section of the heat exchanger, as presented in figure 3. The mean PCM volume temperature is calculated, every time-step, as the average of the sixteen values acquired from the thermocouples.

The PCM fluid's initial temperature is 25ºC. It increases over time through the injection of energy from the HTF and starts the phase change. Figure 4 presents the PCM average temperature in the symmetry axis, for both numerical (present work) and experimental (Hosseini et al., 2014)) data. The model uncertainties are also provided.

It is noticeable in Fig. 4 a good agreement of the data during the first 6000 seconds and the maximum temperature difference of 4.09ºC during the last 3000 seconds. These results outside the uncertainty range occur due the lack of precision of the PCM properties calculations during the charging process simulation. Through these results, the numerical model is assumed as valid and thereby the comparison with other heat exchanger configurations was able to proceed.

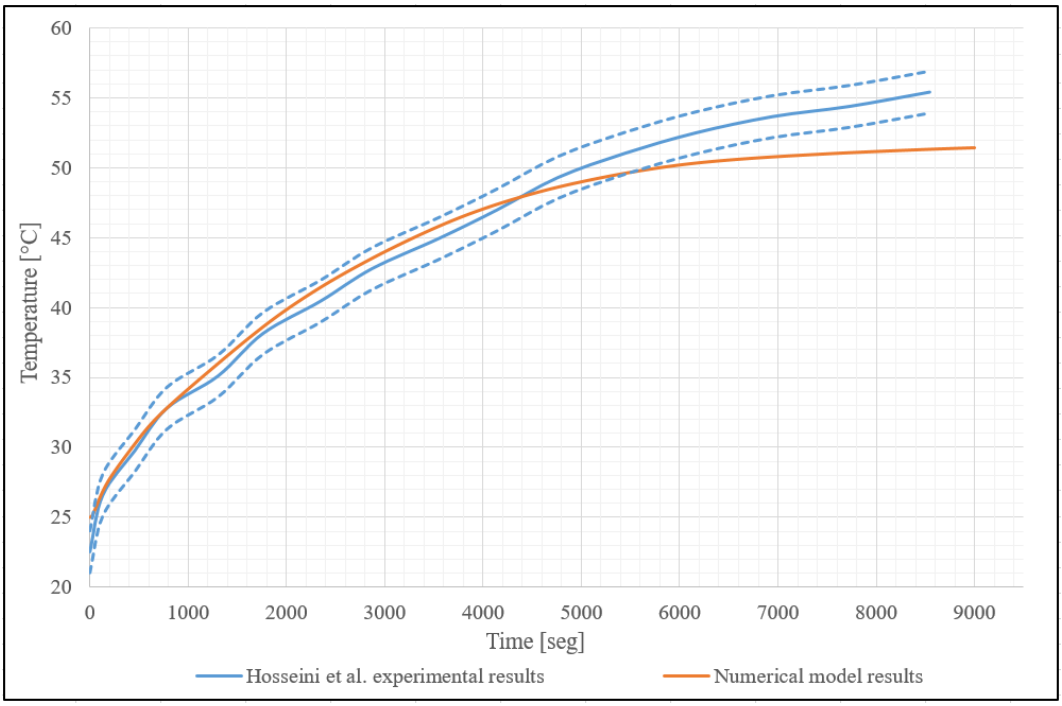

Figure 4. PCM mean temperature results from the experimental and numerical model.

The PCM fusion analysis is investigated using contour plots. Figure 5 showed the cross-section in the YZ plane of the smooth tube heat exchanger (worst performance) and the heat exchanger using circular fins (best performance) at 200 mm away from the HTF inlet over time.

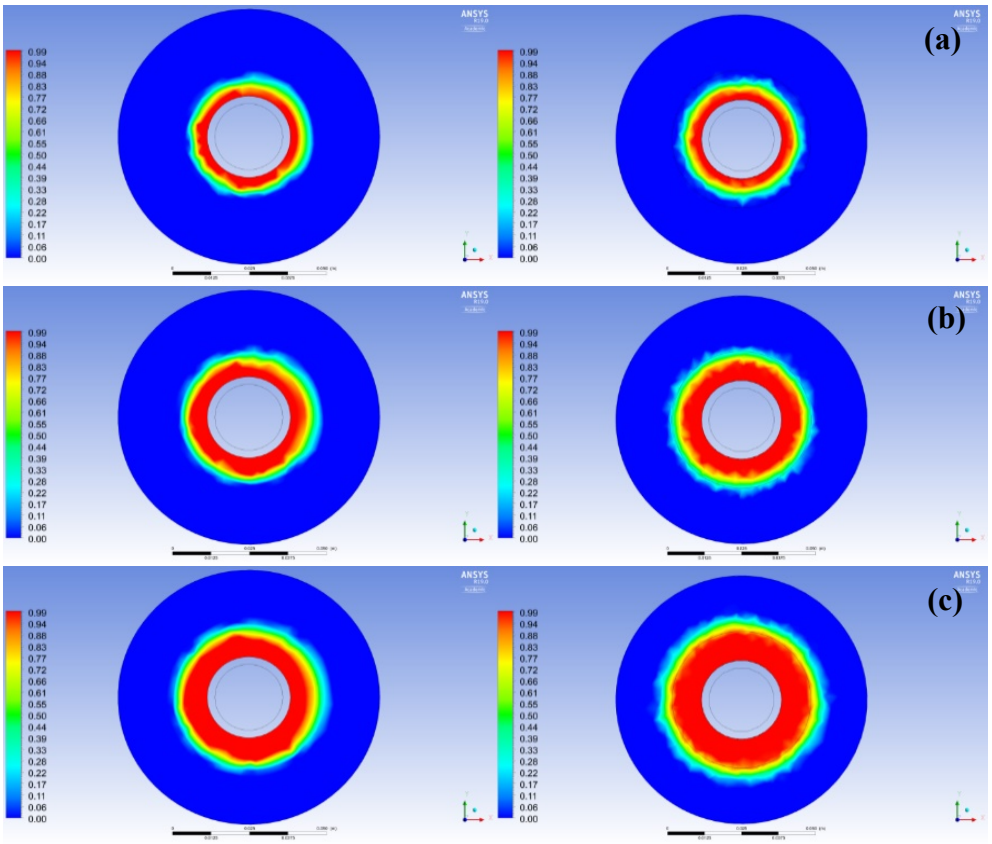

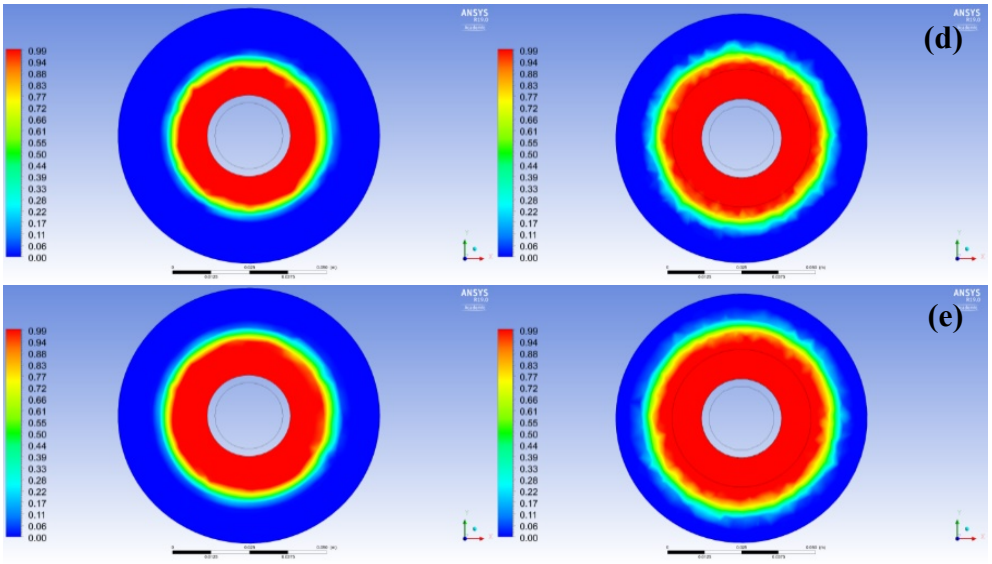

Figure 5. Front view of the smooth tube heat exchanger on the left and of the heat exchanger using circular fins on the right at the instants: (a) 1800, (b) 3600, (c) 5400, (d) 7200, and (e) 9000 seconds.

By 1800 seconds, the smooth tube heat exchanger melts only 8.47%, while the circular fin heat exchanger, 14.11%. After 5400 seconds, the smooth tube exchanger is able to melt 21.15%, while the tube exchanger with circular fins, 34.15%. The circular finned tube heat exchanger has a larger contact area with the PCM compared to the smooth tube exchanger, because of the fins insertion. Thus, it can transfer a greater amount of heat. This fact makes the material reach its melting temperature in less time, making noticeable the portion of liquid PCM expanding faster for the circular finned tube heat exchanger.

The main objective of the heat exchanger applied as LHTES unit is to evaluate its energy storage potential, i.e. its PCM fusion capacity and the energy injected by the HTF. Figure 6 shows the progress of the PCM liquid fraction to 18000 seconds, for the three heat exchanger models.

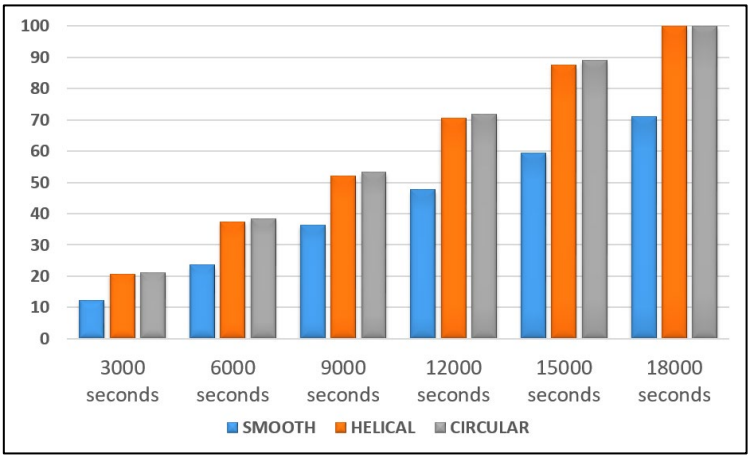

Figure 6. PCM liquid fraction expected progress based on linear regression.

The circular fins significantly increase the heat exchanger contact surface and thus its performance, causing, after 9000 seconds, the fusion of 53.2% of all PCM contained in the space between the shell and the tube. The exchanger using the helical fin presented a slightly lower result, being able to melt 52% of PCM. The smooth tube heat exchanger proves to be the least efficient, melting only 36.44% of PCM at the end of the numerical simulation. Because of that, it is possible to affirm that the circular finned heat exchanger presents the best performance.

After about 2000 seconds, the evolution of the PCM liquid fraction shows a linear behavior. Therefore, a linear regression is performed using Excel software, seeking to estimate the future values of liquid fraction. It is exposed in Figure 6 a very similar performance of the finned tubes heat exchangers, but the circular finned tube heat exchanger presents a slightly better performance, reaching 100% of liquid PCM in 16932 seconds, while the helical finned tube heat exchanger expects to melt the whole PCM in 17242 seconds. The smooth tube heat exchanger, on the other hand, could only achieve 100% molten PCM in 25415 seconds.

5. CONCLUSIONS

The present and future energy demand encourages the study of energy storage systems. By means of that, this work investigates a LHTES system through CFD analysis. The unit, based on a shell-and-tube heat exchanger, is analyzed during a 9000-second simulation for the charging process employing a smooth tube, helical finned tube, and circular finned tube. ANSYS Fluent 19.0 is selected as the software to solve the governing equations and perform the system simulation.

The numerical model validation is made comparing the results generated from the simulation of the smooth tube with the experimental data acquired from the literature. The analysis showed a good agreement during the first 6000 seconds of simulation, but during the last 3000 seconds, it presented a small deviation of 4.09ºC, which confirms the feasibility of the developed numerical model.

The smooth tube heat exchanger was able to make the PCM reach a mean temperature of 51.3°C and melt only 36.44% of the PCM at the end of 9000 seconds. With the improved outer surface by the application of circular and helical fins, the heat exchanger showed a better performance. The finned tube heat exchangers showed very similar mean temperature PCM results, but when the PCM liquid fraction is compared, the circular finned tube heat exchanger obtained slightly better results. The helical finned tube heat exchanger melted about 52% of PCM while the circular finned tube heat exchanger achieved about 53.20% of PCM melted.

At last, it is possible to state that the heat exchanger using a circular finned tube is ideal for practical applications, due to the ability to melt larger portions of PCM in a shorter time, and because of its less complex geometry when compared with the helical finned tube, it is easier to be manufactured.

6. ACKNOWLEDGEMENTS

This study was financed in part by the Coordenação de Aperfeiçoamento de Pessoal de Nível Superior - Brasil (CAPES) - Finance Code 001. The authors are also thankful to CNPq, FAPEMIG and PUC Minas.

7. REFERENCES

Abdulateef, A.M., Mat, S., Sopian, K., Abdulateef, J., and Gitan, A.A., 2017, Experimental and computational study of melting phase-change material in a triplex tube heat exchanger with longitudinal/triangular fins: *Solar Energy*, v. 155, p. 142–153.

Bai, F., Wang, Y., Wang, Z., Sun, Y., and Beath, A., 2015, Economic Evaluation of Shell-and-tube Latent Heat Thermal Energy Storage for Concentrating Solar Power Applications: *Energy Procedia*, v. 69, p. 737–747.

Bhamare, D.K., Rathod, M.K., and Banerjee, J., 2020, Numerical model for evaluating thermal performance of residential building roof integrated with inclined phase change material (PCM) layer: *Journal of Building Engineering*, v. 28, no. May 2019, p. 101018.

Cabeza, L.F., Castell, A., Barreneche, C., De Gracia, A., and Fernández, A.I., 2011, Materials used as PCM in thermal energy storage in buildings: A review: *Renewable and Sustainable Energy Reviews*, v. 15, no. 3, p. 1675–1695.

Cabezas-Gómez, L., Navarro, H.A., Sáiz-Jabardo, J.M., Hanriot, S.D.M., and Maia, C.B., 2012, Analysis of a new cross flow heat exchanger flow arrangement - Extension to several rows: *International Journal of Thermal Sciences*, v. 55, p. 122–132.

Cárdenas, B., and León, N., 2013, High temperature latent heat thermal energy storage: Phase change materials, design considerations and performance enhancement techniques: *Renewable and Sustainable Energy Reviews*, v. 27, p. 724–737.

Crespo, A., Barreneche, C., Ibarra, M., and Platzer, W., 2019, Latent thermal energy storage for solar process heat applications at medium-high temperatures – A review: *Solar Energy*, v. 192, no. October 2017, p. 3–34.

da Cunha, S.R.L., and de Aguiar, J.L.B., 2020, Phase change materials and energy efficiency of buildings: A review of knowledge: *Journal of Energy Storage*, v. 27, no. November 2019.

Fadl, M., and Eames, P.C., 2019, An experimental investigation of the heat transfer and energy storage characteristics of a compact latent heat thermal energy storage system for domestic hot water applications: *Energy*, v. 188, p. 116083.

Fornarelli, F., Camporeale, S.M., and Fortunato, B., 2019, Simplified theoretical model to predict the melting time of a shell-and-tube LHTES: *Applied Thermal Engineering*, v. 153, no. February, p. 51–57.

Fornarelli, F., Camporeale, S.M., Fortunato, B., Torresi, M., Oresta, P., Magliocchetti, L., Miliozzi, A., and Santo, G., 2016, CFD analysis of melting process in a shell-and-tube latent heat storage for concentrated solar power plants: *Applied Energy*, v. 164, p. 711–722.

Gorzin, M., Hosseini, M.J., Rahimi, M., and Bahrampoury, R., 2019, Nano-enhancement of phase change material in a shell and multi-PCM-tube heat exchanger: *Journal of Energy Storage*, v. 22, no. December 2018, p. 88–97.

Guo, S., Zhao, J., Wang, W., Yan, J., Jin, G., and Wang, X., 2017, Techno-economic assessment of mobilized thermal

energy storage for distributed users: A case study in China: *Applied Energy*, v. 194, p. 481–486.
Hosseini, M.J., Rahimi, M., and Bahrampoury, R., 2014, Experimental and computational evolution of a shell and tube heat exchanger as a PCM thermal storage system: *International Communications in Heat and Mass Transfer*, v. 50, p. 128–136.
International Energy Agency, 2019, CO2 Emissions from Fuel Combustion, IEA, 2019.:
Launder B. E., and B., S.D., 2013, MAN - ANSYS Fluent User' s Guide Releasde 15.0: *Knowledge Creation Diffusion Utilization*, v. 15317, no. November, p. 724–746.
Li, H., Wang, W., Yan, J., and Dahlquist, E., 2013, Economic assessment of the mobilized thermal energy storage (M-TES) system for distributed heat supply: *Applied Energy*, v. 104, p. 178–186.
Mehta, D.S., Solanki, K., Rathod, M.K., and Banerjee, J., 2019, Influence of orientation on thermal performance of shell and tube latent heat storage unit: *Applied Thermal Engineering*, v. 157, no. May, p. 113719.
Niezgoda-Zelasko, B., 2016, The Enthalpy-porosity Method Applied to the Modelling of the Ice Slurry Melting Process during Tube Flow: *Procedia Engineering*, v. 157, p. 114–121.
Nitsas, M., and Koronaki, I.P., 2021, Performance analysis of nanoparticles-enhanced PCM: An experimental approach: *Thermal Science and Engineering Progress*, v. 25, no. March, p. 100963.
Obiwulu, A.U., Erusiafe, N., Olopade, M.A., and Nwokolo, S.C., 2020, Modeling and optimization of back temperature models of mono-crystalline silicon modules with special focus on the effect of meteorological and geographical parameters on PV performance: *Renewable Energy*, v. 154, p. 404–431.
Oró, E., Barreneche, C., Farid, M.M., and Cabeza, L.F., 2013, Experimental study on the selection of phase change materials for low temperature applications: *Renewable Energy*, v. 57, p. 130–136.
Pahamli, Y., Hosseini, M.J., Ranjbar, A.A., and Bahrampoury, R., 2017, Effect of nanoparticle dispersion and inclination angle on melting of PCM in a shell and tube heat exchanger: *Journal of the Taiwan Institute of Chemical Engineers*, v. 81, p. 316–334.
Paraffin RT50 - Rubitherm Technologies GmbH Datasheet RT50.:
Permatasari, R., and Yusuf, A.M., 2018, Material selection for shell and tube heat exchanger using computational fluid dynamics method: *AIP Conference Proceedings*, v. 1977, p. 1–7.
Pu, L., Zhang, S., Xu, L., and Li, Y., 2020, Thermal performance optimization and evaluation of a radial finned shell-and-tube latent heat thermal energy storage unit: *Applied Thermal Engineering*, v. 166, no. December 2019, p. 114753.
Qazi, S., 2017, Solar Thermal Electricity and Solar Insolation:
Ruhe, C.H.W., 2019, BP Statistical Review of World Energy: *JAMA: The Journal of the American Medical Association*, v. 225, no. 3, p. 299–306.
Saxena, R., Rakshit, D., and Kaushik, S.C., 2019, Phase change material (PCM) incorporated bricks for energy conservation in composite climate: A sustainable building solution: *Solar Energy*, v. 183, no. March, p. 276–284.
Shen, G., Wang, X., and Chan, A., 2019, Experimental investigation of heat transfer characteristics in a vertical multi-tube latent heat thermal energy storage system: *Energy Procedia*, v. 160, no. 2018, p. 332–339.
United Nations, 2019, WPP2019_POP_F01_1_TOTAL_POPULATION_BOTH_SEXES.:
Versteeg, H.K., and Malalasekera, W., 2007, An Introduction to Computational Fluid Dynamics (Pearson Education Limited, Ed.):
Wang, Z., 2019, Design of the Receiver System:
Waqas, A., and Ji, J., 2017, Thermal management of conventional PV panel using PCM with movable shutters – A numerical study: *Solar Energy*, v. 158, no. October, p. 797–807.
Woolley, E., Luo, Y., and Simeone, A., 2018, Industrial waste heat recovery: A systematic approach: *Sustainable Energy Technologies and Assessments*, v. 29, no. July, p. 50–59.
World Health Organization, 2018, Health, environment and climate change. Road map for an enhanced global response to the adverse health effects of air pollution.: *Seventy-First World Health Assembly*, v. 2016, no. March, p. 1–8.
Yagci, O.K., Avci, M., and Aydin, O., 2019, Melting and solidification of PCM in a tube-in-shell unit: Effect of fin edge lengths' ratio: *Journal of Energy Storage*, v. 24, no. May, p. 100802.
Yang, X., He, L., Xia, Y., and Chen, Y., 2019, Effect of government subsidies on renewable energy investments: The threshold effect: *Energy Policy*, v. 132, no. November 2018, p. 156–166.
Yang, X., Lu, Z., Bai, Q., Zhang, Q., Jin, L., and Yan, J., 2017, Thermal performance of a shell-and-tube latent heat thermal energy storage unit: Role of annular fins: *Applied Energy*, v. 202, p. 558–570.
Yang, X., Sun, L., Yuan, Y., Zhao, X., and Cao, X., 2018, Experimental investigation on performance comparison of PV/T-PCM system and PV/T system: *Renewable Energy*, v. 119, p. 152–159.
Zondag, H.A., de Boer, R., Smeding, S.F., and van der Kamp, J., 2018, Performance analysis of industrial PCM heat storage lab prototype: *Journal of Energy Storage*, v. 18, no. March, p. 402–413.

8. RESPONSIBILITY NOTICE

The authors are the only responsible for the printed material included in this paper.